12-2015

Rainfall interception and the coupled surface water and energy balance

Albert I.J.M. Van Dijk
The Fenner School of Environment & Society

John H. Gash
UK Centre for Ecology & Hydrology

Eva Van Gorsel
CSIRO Oceans and Atmosphere

Peter D. Blanken
University of Colorado Boulder

Alessandro Cescatti
European Commission Joint Research Centre

See next page for additional authors

Rainfall interception and the coupled surface water and energy balance

Albert I. J. M. van Dijk[1*], John H. Gash[2], Eva van Gorsel[3], Peter D. Blanken[4], Alessandro Cescatti[5], Carmen Emmel[6], Bert Gielen[7], Ian Harman[3], Gerard Kiely[8], Lutz Merbold[7], Leonardo Montagnani[9], Eddy Moors[10], Marilyn Roland[6], Matteo Sottocornola[11], Andrej Varlagin[12], Christopher A. Williams[13], Georg Wohlfahrt[14]

[1] Fenner School for Environment & Society, Australian National University, Canberra, Australia

* corresponding author: postal address: Linnaeus way, 0200 Canberra, ACT, Australia. E-mail: *albert.vandijk@anu.edu.au*. Telephone: (+61 02) 612 52197;

[2] Centre for Ecology and Hydrology, Wallingford, UK

[3] CSIRO Oceans and Atmosphere Flagship, Canberra, Australia

[4] Department of Geography, University of Colorado at Boulder, Boulder, USA

[5] European Commission, Joint Research Centre, Institute for Environment and Sustainability, Ispra, Italy

[6] Department of Environmental Systems Science, Institute of Agricultural Sciences, ETH Zurich, Zurich, Switzerland

[7] University of Antwerp, Wilrijk, Belgium

[8] Civil and Environmental Engineering Dept., and Environmental Research Institute, University College Cork, Ireland

[9] Faculty of Science and Technology, Free University of Bolzano, and Forest

Services, Autonomous Province of Bolzano, Bolzano, Italy

[10] Alterra Wageningen UR, Netherlands

[11] Department of Science, Waterford Institute of Technology, Waterford, Ireland

[12] A.N. Severtsov Institute of Ecology and Evolution, Russian Academy of Sciences, Moscow, Russia

[13] Graduate School of Geography, Clark University, Worcester, USA

[14] Institute of Ecology, University of Innsbruck, Innsbruck, Austria

Abstract

Evaporation from wet canopies (*E*) can return up to half of incident rainfall back into the atmosphere and is a major cause of the difference in water use between forests and short vegetation. Canopy water budget measurements often suggest values of *E* during rainfall that are several times greater than those predicted from Penman-Monteith theory. Our literature review identified potential issues with both estimation approaches, producing several hypotheses that were tested using micrometeorological observations from 128 FLUXNET sites world-wide. The analysis shows that FLUXNET eddy-covariance measurements tend to provide unreliable measurements of *E* during rainfall. However, the other micrometeorological FLUXNET observations do provide clues as to why conventional Penman-Monteith applications underestimate *E*. Aerodynamic exchange rather than radiation often drives *E* during rainfall, and hence errors in air humidity measurement and aerodynamic conductance calculation have considerable impact. Furthermore, evaporative cooling promotes a downwards heat flux from the air aloft as well as from the biomass and soil; energy sources that are not always considered. Accounting for these factors leads to *E* estimates and modelled interception losses that are considerably higher. On the other hand, canopy water budget measurements can lead to overestimates of *E* due to spatial sampling errors in throughfall and stemflow, underestimation of canopy rainfall storage capacity, and incorrect calculation of rainfall duration. There are remaining questions relating to horizontal advection from nearby dry areas, infrequent large-scale turbulence under stable atmospheric conditions, and the possible mechanical removal of splash droplets by such eddies. These questions have implications for catchment hydrology, rainfall recycling, land surface modelling, and the interpretation of eddy-covariance measurements.

Keywords: rainfall interception; wet canopy evaporation; FLUXNET; water use; evapotranspiration; Penman-Monteith theory

1. Introduction

Rainfall interception is the fraction of rain that falls onto vegetation but never reaches the ground, instead evaporating from the wet canopy. The most direct way to measure rainfall interception evaporation is through the construction of weighing lysimeters, which is a major undertaking for forests (Dunin et al., 1988). Therefore interception loss (the amount of rainfall lost to wet canopy evaporation) has usually been derived as the residual between event gross rainfall measured above the canopy or in a nearby clearing, and net rainfall, the latter calculated as the sum of separately measured throughfall and stemflow below the canopy. In his pioneering paper, Horton (1919) recognised that *(i)* the fractions of rainfall becoming throughfall and stemflow both vary as a function of storm size and canopy characteristics, *(ii)* canopy water storage capacity, storm duration and the rate of wet canopy evaporation (E in mm h^{-1}) during rainfall are the important variables determining interception loss; *(iii)* the interception process can be conceptualised to consist of two components: wet canopy evaporation during rainfall followed by drying of the canopy once rainfall has stopped; *(iv)* wind can shed water from the canopy, but equally can increase E; and *(v)* in the absence of snow, the fractional interception loss from evergreen vegetation appears stable throughout the year, suggesting that, at least for Horton's site in New York state, USA, event-average rainfall rate (R in mm h^{-1}) and E both increase in summer in approximate proportion. Research since has generally confirmed and refined these observations (see benchmark papers reprinted in Gash and Shuttleworth, 2007). Law (1957) combined throughfall and stemflow measurements with lysimeter drainage measurements to establish a water budget for spruce and pasture. He concluded that the forests had substantially higher rainfall interception losses and, as a consequence, produced less drainage and streamflow.

Nearly a century of further water budget measurements have emphasised the role of vegetation type in determining the magnitude of rainfall interception. Forests typically intercept 10–30% (but sometimes up to half) of the rainfall and rapidly return it to the atmosphere, whereas short vegetation intercepts less rainfall (e.g., Crockford and Richardson, 2000; Horton, 1919; Leyton et al., 1967; Roberts, 1999). This difference goes far in explaining why forest establishment is commonly observed to decrease (and removal increase) streamflow, at least in small catchment experiments (e.g., Van Dijk et al., 2012). However, the physical processes and atmospheric conditions that allow such a large fraction of rainfall to be returned to the atmosphere are poorly understood. In simulation models, rainfall interception is usually estimated in one of two ways (Muzylo et al., 2009): many conceptual hydrological models assume a fixed ratio between 'net' and 'gross' rainfall, without any attempt to reconcile the evaporation rate implied by the water budget (E_{WB}) with the constraint of balancing the energy budget. Alternatively, more detailed process hydrology and land surface models may include a canopy water balance model following the concepts originally introduced by Rutter et al. (1971). These latter models are coupled to the energy balance if they use evaporation rates based on Penman-Monteith theory (E_{PM}).

Numerous studies have combined field measurements of the canopy water budget with sub-daily or event-based interception modelling. By comparing gross and net rainfall for a series of storm events, one can use graphical or regression approaches to derive an ‘effective’ $\overline{E}/\overline{R}$ ratio (i.e., of event-average E and R; cf. Gash, 1979) for multiple events and a mean canopy rainfall storage capacity, S (in mm), where S is defined as the minimum depth of water needed to saturate the canopy. Alternatively, these parameters can be found by fitting the interception model against gross and net rainfall measurements per event (Gash et al., 1995) or time step (Rutter et al., 1971). Less commonly, interception has been estimated by comparing rainfall inputs to changes in total water storage in a column of soil with trees (Dunin et al., 1988). More often than not, the different methods produce results that are difficult to explain in terms of the energy balance, in that inferred E exceeds E_{PM} by a factor of two or more (Holwerda et al., 2012; Schellekens et al., 1999). In other words, the observations cannot be reconciled within a coupled water and energy balance.

The objective of this study is to better understand the reasons for the discrepancy between energy and water balance approaches in determining interception loss. This discrepancy is reflected in the uncertainty of flux estimates; in fact, commonly rainfall interception is not even considered as a separate process in the estimation of evapotranspiration by flux tower eddy covariance measurements, remote sensing and modelling methods alike. Better understanding the coupled water and energy balance during rainfall may also have important ramifications for land-use management and water policies, and for our understanding of the role of forests in the climate system (Bonan, 2008). For example, if the rate of vapour return and the rate of energy withdrawal from the boundary layer are greater than current land surface models predict, this may affect the rainfall generation downwind predicted by weather and climate models (Blyth et al., 1994). This in turn would suggest that the implications of vegetation change for rainfall and water resources availability downwind might need to be reconsidered. Conversely, if the true evaporative flux is much lower than estimated from field measurements, it might require a revision of currently held assumptions about the impact of land-cover change on the catchment water balance.

Several hypotheses have been proposed to explain the discrepancy between water budget and energy balance methods, but to the best of our knowledge they have not been systematically assessed or tested. This was the primary motivation for this study.

This article is structured as follows. The theoretical framework to analyse the energy balance theory during rainfall is provided in Section 2. The global FLUXNET ‘La Thuile’ database (Baldocchi, 2008; Baldocchi et al., 2001) provided unique opportunities to test several of the hypotheses. Details on data selection and the list of 128 sites are provided in Annex A, whereas methodological challenges in measurement and data processing are discussed in Section 3. The proposed causes for the discrepancy in estimated wet canopy evaporation rates are identified in Section 4, and subsequently tested in the following sections. Specifically, issues in applying Penman-Monteith theory are investigated in Section 5, whereas issues in the application of rainfall interception models are examined in Section 6. Finally, we summarise our main conclusions in Section 7. Each hypothesis tested required its own data analysis with a varying level of methodological complexity.

To maintain readability we described the data analysis methods and results together, and relegated some more intricate aspects of the methodology to appendices B (canopy heat flux estimation) and C (simplified rainfall interception model).

2. Theory

Rutter (1967) was the first to apply the Penman (1952) equation to rainfall interception. With later modifications introduced by Monteith (1981), the Penman-Monteith equation can be used to estimate latent heat flux, λE (W m^{-2}) as:

$$\lambda E_{PM} = \frac{\Delta}{\Delta + \gamma'} A + \frac{\rho c_p}{\Delta + \gamma'} g_a (e_s - e) \tag{1a}$$

with

$$\gamma' = \gamma(1 + g_a / g_s). \tag{1b}$$

where Δ (Pa K^{-1}) is the slope of the saturation water vapour pressure curve at air temperature T (K), γ' and γ (Pa K^{-1}) are the adjusted and original psychrometric constants, A (W m^{-2}) is the available energy, ρ (kg m^{-3}) the specific density of air, c_p (J kg^{-1} K^{-1}) the specific heat of air at constant temperature, g_a and g_s (m s^{-1}) the aerodynamic and surface conductances, respectively, while the difference between saturation vapour pressure at ambient temperature e_s (Pa) and the actual vapour pressure e (Pa) is the vapour pressure deficit or VPD. Rutter (1967) pointed out that for a wet canopy, the latent heat flux is no longer limited by stomatal conductance. Therefore g_s should approach infinity and γ' becomes numerically equal to γ. It is noted that in a partially wet but poorly ventilated canopy, surface conductance may still be finite, as found for Amazonian rainforest by Czikowsky and Fitzjarrald (2009). The available energy A is given by (all in W m^{-2}):

$$A = R_n - G - Q \tag{2}$$

where R_n is net all-wave radiation, G is the ground heat flux and Q is the sum of all minor energy sources and sinks, including any change in heat storage in the canopy air, Q_a, and in the biomass, Q_v, as well as energy used for photosynthesis and produced by other metabolic processes. The last two terms are ignored in the present context, but the fluxes Q_v and Q_a may not be negligible, as will be discussed.

Net radiation R_n is typically small during rainfall, because of cloud cover during the day and because rain can equally occur during the night. Rutter (1967) found that wet canopy evaporation could be about four times greater than transpiration rates would have been under the same atmospheric conditions. Importantly, he recognised that the latent heat flux associated with evaporation on days with rain exceeded A and concluded that "*energy is obtained from the air*"; in other words, there is a downwards sensible heat flux (H) and/or cooling of the ambient air. This situation is also predicted by the Penman-Monteith equation if the aerodynamic component of λE_{PM} (the second term) is greater than the radiation component (the first term), since the energy balance $A=H+\lambda E$ demands that (cf. Eq. (1a)):

$$H_{PM} = A - \lambda E = \frac{\gamma'}{\Delta + \gamma'} A - \frac{\rho c_p}{\Delta + \gamma'} g_a (e_s - e) \quad (3)$$

Furthermore, using the bulk aerodynamic approach of Eq. (1a), H is also given by (cf. Penman, 1952):

$$H = \rho c_p g_a (T_s - T) \quad (4)$$

where T_s (K) is the temperature of the surface (e.g., the canopy). A downward sensible heat flux requires that the surface is cooler than the air (Eq. (4)). Pereira et al. (2009) demonstrated that, at least under conditions of low irradiance, the wet crowns of isolated trees cool to temperatures very close to wet bulb temperature, implying that the effective g_s is indeed very high (cf. Eqs. (1a and b). Rutter (1967) measured that wet leaves were up to 1 K cooler than the air above. In turn, the air above the wet canopy was itself on average 1K cooler than at a reference climate station nearby, suggesting that the greater aerodynamic roughness of the forest led to greater evaporative cooling. This was initially dismissed as a forest edge effect, until Stewart (1977) presented measurements over an extensive forest area that also showed a negative H of up to about 50 W m^{-2}. The FLUXNET database also bears this out. Table 1 lists average values of H reported for a wide range of sites in the FLUXNET data base, measured by three-dimensional anemometers. Although reported H values during rain events need to be interpreted with some caution (see Section 3), the average H for all periods with rainfall was negative for 80% of sites (N=108), with an average H of -12 ± 16 W m^{-2} for sites with tall vegetation (>3 m, N=59) and -6 ± 8 W m^{-2} for sites with short vegetation (>1.5 m, N=49; Table 1). The greatest negative H (-31 W m^{-2}) was determined also for the tallest forest (AU-Wac, 70 m tall).

[TABLE 1 HERE]

Because of the typically negative *H*, Stewart (1977) suggested that large-scale advection must occur, which he argued could have been supplied from adjoining land areas with a dry canopy. Alternatively, Shuttleworth and Calder (1979) argued that the lack of surface control and the strong atmospheric coupling of a wet forest canopy means that high *E* can be sustained by "*the considerable sensible heat already stored, or presently being released by the precipitation process, in the lower levels of the atmosphere*". They also commented that sensible heat advection will be common under such conditions, and point out that when there is little radiation, the mere fact that saturation deficits in and near the wet canopy are greater than zero *in itself* provides proof that sensible heat is supplied. Finally, they argue that the occurrence of cloud formation and rainfall is necessarily associated with vertical air mass movement and associated advection.

Since the 1970s, some of these important insights appear to have faded from the collective conscience. For example, the majority of land surface models use conventional Penman-Monteith theory in a way that tends to predict rainfall interception losses that are lower than field experimental knowledge suggests, with unknown consequences for weather and climate modelling. Similarly, methods to estimate total evapotranspiration from remote sensing usually appear to ignore the unresolved wet canopy energy balance problem, and indeed frequently ignore rainfall interception loss altogether; Guerschman et al. (2009) and Miralles et al. (2010) are exceptions.

3. Eddy-covariance measurement during rainfall

In the last few decades, eddy-covariance techniques have provided increasingly sophisticated and widespread measurements of ecosystem-level land surface-atmosphere fluxes, including λE and *H*. The theory underpinning eddy-covariance analysis can be found elsewhere (e.g., Aubinet et al., 2012) but, essentially, it relies on analysing the covariance between high-frequency observed vertical air movement and scalar concentration. Measurements are made with sonic three-dimensional anemometers co-located with open- or closed-path infrared gas analysers. In theory, eddy-covariance measurements could be used to independently verify *E*. However, there does not appear to be consensus, or indeed much published research at all, on the validity of standard eddy-covariance measurement and analysis techniques during rainfall, or methods to detect and/or correct the affected flux data. This is perhaps surprising, given the likelihood of erroneous measurements by at least some of the instruments and given that standard data analysis and gap-filling methods and protocols have been developed to deal with a variety of other measurement issues (e.g., Moffat et al., 2007). The lack of such a standard approach may also explain why it is easy to find examples of analyses that either accept latent heat flux measurements during rainfall without question, or replace these using gap-filling strategies that interpolate the data, essentially assuming that flux behaviour is similar to that under dry canopy conditions. Both assumptions introduce potentially very large errors in ET estimates, a particular concern if the resulting longer-term estimates are reported without caveats or even are used to evaluate model ET estimates (Van Dijk and Warren, 2010).

There are good reasons why FLUXNET eddy-covariance measurements may be of questionable validity during rainfall. While many models of sonic anemometers employ hydrophobic material on the sensors and automatic spike removal, water on the sensor surfaces and raindrops falling through the sensor path still affect instrument readings. Mizutani et al. (1997) tested the performance of sonic anemometers in laboratory conditions and found that up to 2.5 mm depth on the sonic sensor head caused wind speed and sensible heat flux measurement errors within 1%. Simulated rainfall intensities less than 10 mm h^{-1} also did not appear to affect measurements much, although higher intensities did. Similar results have been obtained for other sonic anemometer instruments (Cabral et al., 2010; Gash et al., 1999). By contrast, open path gas analysers do not appear to function at all well for water vapour during rainfall. Burba et al. (2010) found that 75% of open path gas analyser data were lost during rainfall conditions. Closed-path analysers with long unheated intake tubes suffer from other measurement errors due to condensation and re-evaporation in the intake tube (so-called frequency loss). The resulting underestimation of latent heat flux can be large and increases exponentially with humidity (Fratini et al., 2012; Ibrom et al., 2007; Mammarella et al., 2009). Czikowsky and Fitzjarrald (2009) used closed-path measurements during and after rainfall over a tropical rainforest, but did not report on the accuracy of the measurements. Measurement errors during rainfall may also explain why a recent synthesis of global FLUXNET eddy-covariance data found that total ET from forests is less than from grasslands under similar climate conditions (Williams et al., 2012), in contrast with catchment studies.

The quality of eddy-covariance heat flux estimates is commonly assessed by calculating the energy balance ratio (EBR), i.e. the sum of λE and H divided by A, for a selected period (Stoy et al., 2013; Wilson et al., 2002). This method does not necessarily work well for wet canopy conditions, as it was shown that λE and H will often have opposite signs (i.e., an upwards latent and downwards sensible heat flux). Temporarily assuming Q=0 (i.e., A=R_n–G; cf. Eq. (2)), energy balance calculations for the FLUXNET sites suggest an average 'missing' energy loss under dry conditions of 16 ± 13 W m^{-2} for tall and 11 ± 13 W m^{-2} for short vegetation, producing mean EBR values of 80% and 86%, respectively (Table 1). However, during wet conditions, the situation degrades with missing fluxes of 28 ± 20 W m^{-2} for tall and 18 ± 17 W m^{-2} for short vegetation, producing respective EBR values of -37% (note the negative sign) and 36%. These numbers get considerably worse if Q is accounted for (see Section 5.2), suggesting that λE derived from FLUXNET eddy-covariance measurements during and shortly after rainfall are too low.

Alternatively, some studies have avoided gas analyser measurements *during rainfall* by calculating λE as the energy balance residual, i.e., λE=A–H. Following this approach, Herbst et al. (2008) calculated E that could be reconciled with E_{PM} as well as with E_{WB}. However, Van der Tol et al. (2003) did not find good agreement. We calculated λE as the energy balance residual for the FLUXNET data, again temporarily ignoring Q. For sites with tall vegetation, this produced an average value of 45±18 W m^{-2} instead of the 17±15 W m^{-2} listed in Table 1. For short vegetation, the average latent flux was 35±17 W m^{-2} instead of the reported 17±14 W m^{-2}. However, it is not clear if it is appropriate to assume that all energy balance errors simply can be attributed to λE to produce a reliable estimate (Foken, 2008). In particular, the importance of low frequency turbulence in the commonly stable atmospheric conditions during rainfall is unknown. The influence of low frequency flux contributions in eddy-covariance data processing can be problematic. The measured covariance is usually split into the product of means (interpreted as the advection term) and the fluctuations (the eddy fluxes) by 'block time averaging', commonly for 30 minute intervals (Finnigan et al., 2003). However, Sakai et al. (2001) found that eddies with a return interval of more than 40 minutes can contribute to up to 40% of surface fluxes during light wind conditions around midday over a temperate forest. This means that 30-minute time block-averaging can introduce substantial errors and lead to underestimates of H. This in turn would mean that the 'real' energy balance residual, and therefore λE, would be greater than calculated. Overall, therefore, FLUXNET eddy-covariance flux data during rainfall and shortly thereafter need to be treated as suspect.

4. Proposed causes for the discrepancy in estimated wet canopy evaporation rates

The most common way to determine E is via a canopy water budget, where rainfall is measured above the canopy, and throughfall and stemflow beneath it. Gross rainfall measurements can be affected by the influence of the gauge itself on the wind field; Sevruk (2006) suggests a typical systematic under-catch of ca. 2-10%, depending on height above the surface or canopy. However, an over-catch in gross rainfall measurement would be needed to explain the inferred high rainfall interception rates. This may occur where gauges are placed in sheltered locations, e.g., in a gap within a forest (see Sevruk, 2006 for further discussion).

Spatial throughfall and stemflow sampling errors can lead to overestimation, but more commonly, underestimation of throughfall and stemflow, depending on the vegetation structure and the way it affects the occurrence of drip points and funnelling of excess water from the canopy (Holwerda et al., 2006; Lloyd and Marques, 1988). In some experimental studies, stemflow has been ignored altogether. Stemflow usually represents less than 2% of the canopy water balance, but in extreme cases it can amount to more than 10% of total rainfall (Levia and Frost, 2003; Llorens and Domingo, 2007). Experimental design and sampling issues can explain some of the high rainfall interception rates inferred, and will usually lead to an overestimation of interception. However, carefully designed water budget studies with a large number of roving throughfall gauges and measurements of stemflow still tend to find higher interception rates than predicted from E_{PM} (e.g., Holwerda et al., 2006). Thus, such water budget errors can only provide a partial explanation.

Other hypotheses can be categorised in different ways. Several hypotheses question the validity of the E_{PM} estimates, or at least the assumptions made or data used, if not Penman-Monteith theory itself. Others address possible errors arising from the explicit or implicit assumptions in the rainfall interception models (Table 2). These are discussed in the next two sections.

[TABLE 2 HERE]

5. Errors in applying Penman-Monteith theory

The Penman-Monteith theory invokes a number of assumptions. Predominantly these are that (1) all transport terms (of energy and water) are accounted for; (2) the site can be considered horizontally homogeneous; and (3) that the flow is statistically horizontally homogeneous and stationary. These three assumptions allow evaporation to be modelled as a one-dimensional system and ensure consistency through time of the relationships between the measurable meteorological variables, the fluxes of interest and the model coefficients, especially with the aerodynamic conductance. Each assumption, however, can be challenged by the specifics of the site and the rainfall event.

5.1. Unaccounted energy advection

Shuttleworth and Calder (1979) observed that unexpectedly high E appeared to occur mainly at maritime sites, whereas interception measured at locations further inland were more in line with E_{PM}. This led to the hypothesis that horizontal advection of sensible heat from the ocean could provide a source of additional energy not accounted for in the conventional use of the Penman-Monteith model. Further evidence of a maritime influence was later found by Schellekens et al. (1999). Advection of energy from the ocean requires an onshore wind that brings in air with a higher temperature and/or VPD, or both. Roberts et al. (2005) suggested that such a process is unlikely for most locations as it would require a horizontal temperature gradient of several K per 100 m (although they did not present the calculation). Moreover, a locally generated ‘sea breeze’ would normally bring in cooler and moister air rather than warmer and drier air, and therefore a large-scale synoptic mechanism would be required. However, advected energy does not need to come from the ocean: particularly under convective conditions there will be warmer and drier air available from nearby areas without rain (Stewart, 1977). Energy advection does not invalidate Penman-Monteith theory, but energy advected horizontally *below* the level of (vertical) energy balance measurement would be unaccounted for. This normally occurs only on the edges between contrasting surfaces, although strong convective storm cells may also draw in air laterally. On the other hand, vertical energy advection from the higher boundary layer should still be measured as a negative H and reflected in air temperature and humidity.

Alternatively, Holwerda et al. (2012) argued that the previously postulated maritime-continental contrast may have been misinterpreted and that high E may in fact be a feature of enhanced topographic roughness and exposure in complex, mountainous terrain, which happened to coincide with proximity to the ocean in previous studies. The increased relief enhances boundary-layer mixing compared to flat terrain and creates local variations in wind speed depending on wind direction and, potentially, lateral advection of energy below the eddy covariance instruments. Numerical and theoretical studies demonstrate that the deviations in air flow and turbulence in the boundary layer, as it responds to even minor topography, challenge many of the assumptions underpinning both Penman-Monteith and eddy covariance theory (e.g., Raupach and Finnigan 1997, Huntingford et al. 1998, Finnigan 2004). These issues are even more severe where there is a tall canopy, which generates multiple interactions between the turbulence and the terrain-induced circulation (Finnigan and Belcher 2004, Belcher et al. 2008, 2012, Ross 2014). The impacts of these processes are contingent on the specifics of the site and the rain event, and therefore in conclusion, it would seem unlikely that advection alone can explain why E_{PM} estimates should be systematically too low.

5.2. Underestimation of biomass and ground heat release

Release of thermal energy stored in the forest, both in the vegetation biomass (Q_v) and in the air below the measurement level (Q_a), may also provide an additional source of energy for evaporation (Moors, 2012). These heat fluxes can be estimated by considering the pre-storm air temperature, the structure and dimensions of the biomass elements and their surface temperature, which for a wet canopy may be assumed to be intermediate between air temperature and wet bulb temperature, depending on ventilation. Michiles and Gielow (2008) measured forest heat storage changes in an Amazonian rain forest and found that it could contribute as much as 200 W m^{-2} due to rapid cooling of the forest. Such a high heat flux is presumably limited to the beginning of a storm and unlikely to be sustained for a prolonged period. Where forest heat storage has been estimated, it typically represents a very small flux over the duration of an entire storm (Gash et al., 1999; Pereira et al., 2009). Q can be simulated using physical models that require detailed knowledge of forest structure, biomass and physical properties (Haverd et al., 2007; Kobayashi et al., 2012). We did not have access to such observations for the numerous sites, and therefore used a simplified method to obtain an order of magnitude estimate of Q (see Appendix B). The resulting estimates of Q are an average release of 29 ± 31 W m^{-2} during rainfall periods for sites with tall vegetation (>3 m, N=59), and a (negligible) 0.8 ± 1.3 W m^{-2} for sites with short vegetation (<1.5 m, N=49). For tall vegetation, this means that Q is typically larger than H (-12 ± 16 W m^{-2}) and of similar magnitude to R_n (31 ± 22 W m^{-2}). In other words, it is an important source of evaporative energy. The biomass heat flux Q_v is responsible for an average 93% of total Q across sites, primarily because Q_a is the net result of the counteracting effects of cooling air temperature and increasing moisture content (Eq. (A.1)). The overall Q was largely explained by the estimated rate of biomass temperature change (-1.6 K h^{-1} on average) and the height of the vegetation; their product explained 99% of the variance in total Q (cf. Eq. (B.2)). The site with the highest average Q during rainfall periods (222 W m^{-2}) was also the tallest forest in the database (AU-Wac). Unfortunately, the accuracy of Q estimates could not be tested. Given the assumptions about surface temperature, it probably represents an upper estimate. Accounting for Q resulted in an increase in λE_{PM} for tall vegetation from 82 ± 86 W m^{-2} to 108 ± 102 W m^{-2}; i.e. a modest increase of 17%.

An upward ground heat flux (G) may also be expected during rainfall. In theory, this could add energy to the canopy air and so potentially help increase evaporation. Values of G reported in the FLUXNET database suggest an average upward heat flux of 2 ± 8 W m^{-2} for tall vegetation, representing 8% of R_n. For short vegetation, the average upward heat flux is 6 ± 11 W m^{-2}, equivalent to 28% of R_n. (It is noted that G reported in the FLUXNET database is often derived from heat flux plates and may not always account for heat storage in the soil above the flux plate). It follows that G might be a modest but arguably non-negligible source of evaporative energy during rainfall.

5.3. Errors in air humidity measurement

Calculating E_{PM} requires observations of VPD during rainfall. In the FLUXNET data, this is most commonly calculated from relative humidity (RH) measured by capacitor sensors, but these are not sensitive in humid air and can be affected by rain splash and condensation on the radiation shields. This can have considerable influence on E_{PM} estimates through Eq. (1). For example, Wallace and McJannet (2006) calculated that a 2% RH reduction can increase E_{PM} by 31%. The reported mean RH during rainfall was 90±5% across the FLUXNET sites compared to 72±11% during dry periods. To assess the influence of RH errors, E_{PM} was calculated using the observed RH as well as with RH reduced by 2%, simulating the effect of a systematic bias. Reducing relative humidity by 2% inevitably increased estimated λE_{PM}, by an average 34 ± 23 % across sites, or from an average 72 ± 78 to 92 ± 76 W m^{-2} across all sites (N=108). The variation was large, however, with a maximum relative increase of 2.3 times for one site (US-FPe), from 7 to 19 W m^{-2}. We cannot assess whether there might be a systematic bias in the RH values reported in the FLUXNET database; systematic evaluation against a more accurate sensor during rainfall would be required (e.g., using a cooled mirror dew point hygrometer; cf. Schmidt et al., 2012). An apparent drift in annual maximum relative humidity of a few percent over several years has been observed for some FLUXNET sites, suggesting that such errors are certainly conceivable (Dr. M. Sottocornola, pers. comm.).

5.4. Underestimation of aerodynamic conductance

Vertical air exchange is important during wet canopy conditions, as E is driven by aerodynamic energy and the associated downward H. Dunin et al. (1988) analysed forest water storage changes measured by a weighing lysimeter and hypothesised that updrafts during storms might be responsible for the high E they inferred from the lysimeter water budget. Particularly before the onset and during the early stages of a thunderstorm, strong updrafts can occur depending on the convective power of the storm. Complex terrain typically enhances boundary-layer mixing compared to flat terrain and imposes terrain-scale variation to the aerodynamic conductance (e.g. Raupach and Finnigan 1997). . Other researchers also highlight the importance of site exposure to wind (e.g., Van Dijk and Bruijnzeel, 2001b). Both convective and orographic updrafts would seem potentially efficient mechanisms to transport moisture and enhance E by drawing in drier and/or warmer air, laterally or from higher up in the atmosphere, or both. They also challenge the assumption of consistency in the bulk-aerodynamic relationship, however.

All the above processes may enhance vertical air exchange, and hence increase the aerodynamic conductance, beyond that predicted by Monin-Obukhov similarity theory (MOST) (Holwerda et al., 2012). This is a potentially important source of error in E_{PM} calculations, as the usual method to quantify the aerodynamic conductance, and that taken here, assumes a logarithmic wind speed profile based on MOST (Thom, 1975). This estimate of the aerodynamic conductance g_{aT} is determined from the (horizontal) wind speed measured at a reference height as (e.g., Shuttleworth, 2012):

$$g_{aT} = \frac{ku_*}{\ln\left(\frac{z-d}{z_{0s}}\right) - \psi_s} \tag{7}$$

with

$$u_* = \frac{ku_z}{\ln\left(\frac{z-d}{z_{0m}}\right) - \psi_m} \tag{8}$$

where k (0.40) is von Kármán's constant, d (m) the zero displacement length, z_{0m} and z_{0s} (m) the roughness lengths for the transfer of momentum and scalars (i.e., heat and water vapour density), respectively, and ψ_m and ψ_s the stability corrections for momentum and scalar transfer, respectively. The latter are sometimes calculated, but often assumed negligible. The values of d and z_{0m} cannot be determined without wind profile measurements. Following Rutter et al. (1971), it is usually assumed that d=0.75h and z_0=0.1h, where h is the canopy height (but see Gash et al., 1999, for an observation-based approach). (Commonly reported values of z_{0s}/z_{0m} are 1/12 to 1/2. Testing showed that the actual value chosen had little influence and so here we used an intermediate ratio of 1/7.) Furthermore, the adoption of a single z_{0s} for heat and vapour transport implies that they have the same plane of origin and that this origin is fixed, which may not always be the case (Moors, 2012). Errors in any of these assumptions may be particularly important during rainfall: when the surface has a finite surface conductance, g_a will occur both in the numerator and the denominator of the aerodynamic term of the Penman-Monteith equation (Eq (1)) and therefore errors in g_a may not have a large effect, particularly if $g_a >> g_s$. However under wet canopy conditions g_a disappears from the denominator and hence errors in its estimation have more influence.

As three-dimensional wind speed measurements are made at the FLUXNET sites, errors in the application of the above approach may be deduced from a comparison of g_{aT} and g_{aU}. Site values for h and z to calculate g_{aT} were obtained from the primary references (Appendix A), from the site investigators, and from multi-site studies listing these variables (Amiro et al., 2006; Chen et al., 2009; Curtis et al., 2002; Rebmann et al., 2005; Richardson et al., 2006; Stoy et al., 2006; Wang et al., 2008; Wilson et al., 2002). Friction velocity (u_*) can be derived directly from sonic wind speed measurements (Gash et al., 1999) and used to calculate aerodynamic conductance (g_{aU}) with:

$$g_{aU} = \frac{u_*}{\frac{u_z}{u_*} + \frac{1}{k}\ln\left(\frac{z_{0m}}{z_{0s}}\right) - \frac{\psi_s}{k}} \tag{9}$$

The resulting mean g_{aU} and g_{aT} values across all sites are similar, but the relationship between the two is poor (r^2=0.26, Figure 1). This emphasises the assumptions underpinning the two respective methods, and the challenge in predicting the wind speed profile in the case of g_{aT}. The λE_{PM} values calculated with g_{aU} were not systematically higher or lower than those calculated with g_{aT}; on average the former was 1.05 ± 0.37 times greater than the latter. Including the stability correction (following Paulson, 1970) increased g_{aU} by 1.5% on average but increases and decreases both occurred, depending on the dominant sign of H, and changes were small, with extremes of -4% and +6%. It follows that assumptions in the calculation of g_a following Thom (1975) can certainly introduce large errors, but underestimates of λE_{PM} appear about as likely as overestimates.

[FIGURE 1 HERE]

Both approaches to calculate g_a still require MOST to be valid. In addition to the issues raised above and the possibility of systematic advection raised (Section 5.1), there are other reasons why this may not be the case. MOST invokes assumptions concerning the scales characterising the turbulent flow;

specifically, that u_* is the only important velocity scale, and that height (z–d) and the Obukhov length are the important length scales. At several FLUXNET sites, especially those with tall canopies, observations may be taken in the roughness sub-layer. In this layer the turbulence is also characterised by length scales related to the surface. For example, over tall canopies the mixing layer instability that occurs at canopy top (e.g., Raupach et al. 1996) implies that a length scale linked to canopy density needs to be included in the analysis. Typically, the mixing layer instability leads to enhanced turbulent mixing and, correspondingly, g_{aU} and g_{aT} would be expected to underestimate the true aerodynamic conductance. Corrections to MOST for this tall canopy effect have been developed for dry conditions (e.g., Harman and Finnigan, 2007, 2008) but require calibration against site data for accuracy. Furthermore, turbulence during rainfall is additionally impacted through two other processes: the presence of rain droplets provides a large surface area for viscous dissipation, and falling rain imposes a drag on the atmosphere. Both processes add further length scales to the problem, and an appropriate correction method is yet to be developed and demonstrated.

Finally, wind speed u_z needs to be correctly measured. Errors can occur if wind speeds are not measured directly above the canopy, but at a site with less exposure, e.g., in a forest gap or at a less exposed airport or climate station nearby, as is quite common in canopy water budget studies. The wind speed may also be underestimated if the event-average wind speed is assumed equal to daytime or daily average wind speeds on the day, or on dry days, as is a common practice.

In summary, the errors in the estimation of g_a are easily made, can be of considerable magnitude, and have an important influence on E_{PM} estimates.

5.5. Mechanical water transport

Even more difficult to evaluate is the effect of rain splash on the return of water to the atmosphere. Dunin et al. (1988) (see Dunkerley, 2009) and later Murakami (2006) point out that drops falling onto the canopy produce small impact droplets that can remain suspended in the air for long enough to partially or wholly evaporate before reaching the ground. For example, Murakami (2006) calculated that droplets of <50 μm diameter are likely to completely or largely evaporate when falling from a tall forest canopy. Ghadiri and Payne (1988) measured the size distribution of impact droplets formed by a 6 mm diameter drop hitting different surfaces; from the data they tabulate it can be calculated that drops of <1 mm diameter represent at least 10% of the total volume of impacting droplets. Measurements by Bassette and Bussière (2008) show that considerably more than half the volume of a large drop can be scattered in splash droplets when hitting a leaf. The largest number of droplets are produced when large drops are sliced, e.g., on leaf edges or petioles, and while large drops are relatively few in natural rainfall, they are ubiquitous in throughfall dripping through successive layers of the canopy (Dunkerley, 2009). However, the associated increase of the evaporating surface does not necessarily increase the latent heat flux, as surface conductance is already assumed to be infinitely large, whereas the aerodynamic conductance of the canopy should not be affected by the presence of splash droplets. In other words, E is ultimately controlled by the ability of the turbulent boundary layer to transport water vapour away from the surface, rather than by the area of the evaporating surface.

The observation that *(i)* rainfall onto a canopy can produce many small droplets and *(ii)* strong vertical updrafts can occur during rainfall, suggests that updrafts can potentially also play a role in enhancing rainfall evaporation rates. The upwards vertical air movement may slow down sufficiently small impact droplets, or even transport them back into the atmosphere above the rainfall measurement level. This could create further opportunities for the droplets to evaporate, or to be swept up by falling raindrops and return to the surface, to be measured once again as rainfall. The mechanics appear to be feasible, as drops of 0.5 and 1 mm diameter have a maximum fall velocity of only 2 and 4 m s^{-1}, respectively (Gunn and Kinzer, 1949), and updrafts of this strength (equivalent to a gentle breeze) occur frequently in the turbulent conditions associated with thunderstorms, at least above the canopy. Detecting this process may be possible using disdrometer measurements above the canopy, recording water droplet sizes and fluxes in both upward and downward motions down to the scale of fine-scale droplets that can be suspended by eddy motions. The existence of this process would not invalidate E_{PM}, but would add an additional mechanical vertical transport flux. It would go towards explaining the greater difference between rainfall above and below a tall and rough canopy, when compared to shorter vegetation.

5.6 Summary

Based on the foregoing analysis, we can predict the energy balance during rainfall using the Penman-Monteith equation to estimate λE_{PM} and H_{PM} (Eqs. (1–3)), and accounting for Q and G, as well as using measured g_{aU}. The resulting average λE_{PM} is not hugely different from ‘conventional’ Penman-Monteith based estimates (λE_{PMo}), but both are several times larger than the results of eddy-covariance measurements (λE_{EC}) (Table 3). It is noted that downward H_{PM} predicted by Penman-Monteith theory is considerably greater than that derived from the eddy-covariance measurements (Table 3). Moreover, these estimates do not account for several of the identified potential issues, such as humidity measurement errors, horizontal advection below the measurement level, problems using MOST, the influence of infrequent eddies, and mechanical transport.

[TABLE 3 HERE]

6. Errors in applying rainfall interception models

6.1. Underestimation of canopy rainfall storage

When estimating *E* by fitting an interception model to event-total values of interception loss, there can be a degree of functional equivalence (or 'parameter equifinality'; Beven, 1993) between *E* during rainfall and canopy rainfall storage capacity (*S*), from which evaporation may continue after rainfall has ceased. Therefore, underestimation of *S a priori* is likely to be compensated by overestimation of *E*. Because event-total throughfall and stemflow can be measured more easily and cheaply than their instantaneous rates, the event-based analytical rainfall interception model (Gash, 1979; Gash et al., 1995) has been applied more commonly than the dynamic model from which it was derived (Rutter et al., 1971). The event-based analytical rainfall interception model has two particularly important parameters that need to be estimated, *S* and ratio $\overline{E}/\overline{R}$, and due to functional equivalence, an error in one can lead to a compensating error in the other. For example, the graphical envelope method of Leyton et al. (1967) to derive *S* from event gross and net rainfall measurements inevitably leads to underestimates.

Field methods to estimate *S* also have their issues, however. Some have pointed at the large rainfall storage capacity of tree bark and epiphytes (Herwitz, 1985; Wallace and McJannet, 2006), although study of the water balance of epiphyte mosses by Hölscher et al. (2004) demonstrated that their effectiveness in increasing interception losses is limited by the degree to which they dry out in between storms. Similar arguments can be made for other water-retaining materials in the canopy. The implication is that *S* is likely overestimated if the total amount of water that such materials will hold is assumed to evaporate. The importance of assumptions about *S* is revisited in Section 6.3.

6.2. Overestimation of rainfall rate

The correct estimation of E_{WB} from the ratio $\overline{E}/\overline{R}$ is contingent on accurate specification of *R*, and thus an overestimate of *R* could explain why E_{WB} might be overestimated. The Gash model is based on the assumption that the canopy has dried out between events. If the time interval adopted to separate successive storms is too short for this to be true, then effective storm duration will be underestimated and hence *R* and *E* will be overestimated (Wallace and McJannet, 2006). Furthermore, *R* is normally measured with tipping bucket rain gauges that have discrete 0.1–0.5 mm accumulation increments. If *R* per time step is less than this increment, then the instrument will not register rainfall during every time interval and errors in estimated storm duration can result. Storm duration errors can change *R* estimates by more than 50%, given that storm separation times used in the literature can vary from 2 to 6 hours (Wallace and McJannet, 2006). This effect was calculated for all FLUXNET sites with rainfall data. Half hours with rainfall in excess of 0.25 mm were clustered together in one event if they were separated between 0.5 and 24 hours. The overall average rainfall intensity R was calculated as the total rainfall divided by the total duration of all events, including the intra-storm intervals without rainfall (Figure 3a). The reduction in R with increased separation time was similar for all sites; R for 1 hour separation time (R_1) was on average 1.46 times greater than for 6 hour separation time (R_6), varying from 1.14 (US-Wrc) to 2.04 (CA-Obs) times. It follows that assumptions about the time required for the canopy to dry up can indeed have a considerable influence on R. The impact of assuming shorter canopy drying times on estimates of total interception loss is mitigated by the fact that the reduction in evaporation during the event can be partially compensated by an increase in evaporation after the event, as the total number of events will increase if the separation time is shortened (Figure 2b). Underestimating canopy drying time will however still lead to an overestimation of E during rainfall and so can partially explain the discrepancy with E_{PM} estimates.

[FIGURE 2 HERE]

6.3. Insights from rainfall interception modelling

We used a simplified version of the Rutter et al. (1971) model (described in Appendix C) at half-hourly time step to simulate event-based rainfall interception losses for each site. We do not claim that the derived estimates accurately reflect rainfall interception losses for individual sites, as we needed to make assumptions about S and about the canopy cover fraction. Rather, the objective of this exercise was to further investigate the effect of assumed S on simulated interception losses and to investigate the order of magnitude of interception losses obtained when using our best estimate λE_{PM} values. Figure 3 shows the relationship between assumed S and the range of simulated values for interception loss expressed as a percentage of rainfall. This shows that the estimated interception loss is sensitive to the choice of S; interception loss increased approximately proportional to S to the power 0.3 (Figure 3).

[FIGURE 3 HERE]

Values of the minimum amount of water needed to saturate the canopy (S) reported in the literature are typically on the order of 0.5 to 2 mm (e.g., Wallace et al., 2013), but even within this range the choice of value is quite influential. Interception loss estimates for this narrower S range are in the order of 10–50% with an average of ca. 20–30%. These numbers are in fact surprisingly close to interception fractions observed by water budget methods. Of several vegetation and weather variables tested, characteristics related to rainfall event size and intensity were the best predictors of interception loss (in terms of r^2, data not shown), for any assumed value of S. Figure 4 illustrates this using the average depth of rain per rain-day (P_d, i.e. the ratio of annual rainfall over number of days with rain, chosen because it is straightforward to calculate). The scatter in Figure 4 can be attributed mainly to site-to-site variability in E (hence the difference between short and tall vegetation) and to differences in the temporal scaling behaviour of rainfall (e.g., the site US-Wrc represents tall coniferous forest that experiences large storms in terms of total volume but falling with low R). The lowest simulated interception loss was 4-26% (range for different S) for a grassland in Mississippi, USA (US-Goo), experiencing high R (average 3.8 mm h^{-1}) and average E (0.10 mm h^{-1}) during rainfall. The highest simulated interception loss was 27–59% for an evergreen forest in Italy (IT-Ren) experiencing low R (0.45 mm h^{-1}) and average E (0.11 mm h^{-1}).

[FIGURE 4 HERE]

For S=1 mm, the resulting R averaged over the entire event is considerably less than the R calculated for half hours with rainfall only (Table 4). This re-emphasises the point made earlier that event-averaged R will decrease when considering intra-storm periods without rain during which the canopy does not fully dry (Valente et al., 1997). On the other hand, event-average $\overline{E}$ was not significantly different from E during rainfall intervals only (Table 4). The resulting ratios of mean E over mean R were on average 2.05±0.63 times greater than values calculated on the basis of half-hours with rainfall only (range 1.13–4.20). Finally, E during the drying out phase was considerably higher than that during the event, by an average 2.02±0.69 times, although values varied considerably between sites (range 0.61–4.64 times). The corresponding average drying time for S=1 mm was simulated to be 3.9±1.9 hours, but varied as a function of E (1.2–12.2 hours).

[TABLE 4 HERE]

Incidentally, the best predictor of event-average E was VPD (r^2=0.53, N=82), whereas multiplying VPD with g_{aU} or g_{aT} (cf. Eq. (1a)) further increased r^2 to 0.74. This further emphasises the importance of the aerodynamic term of E_{PM}. The contribution of the aerodynamic term in Eq. (1a) can also be calculated directly and contributed an average 61±18 % to total E_{PM} during rainfall periods (N=108). As another aside, the model results presented here can also be used to examine one of the assumptions of the analytical interception model, namely, that the ratio $\overline{E}/\overline{R}$ can be assumed constant over all events. Although this assumption can be argued against on conceptual grounds (greater storms might be presumed to have greater rainfall rates), it generally does not appear to affect model performance negatively. We examined the relationship between storm size P (mm) and $\bar{E}/\bar{R}$ for all individual sites with more than 20 events in excess of 5 mm (N=74). For all but one site, $\bar{E}/\bar{R}$ in fact did decrease with increasing storm size, but more so for small storms (e.g., <5 mm) than for larger ones. Overall, correlation was typically not strong, with an average r^2 of -0.23±0.08. Further examination showed that this was partly because E slightly increased with increasing P, but mainly because R was just not strongly related to P. This explains why the assumption of constant $\bar{E}/\bar{R}$ often still produces good agreement with canopy water budget observations.

7. Conclusions

In this study, we investigated why canopy water budget measurements of rainfall interception almost always suggest wet canopy evaporation rates (E_{WB}) that are several times higher than those predicted from Penman-Monteith theory (E_{PM}). We examined several proposed explanations for this discrepancy by reviewing the literature and examining the FLUXNET database. We summarise our main findings as follows:

[1] Relatively high E can be sustained during rainfall by a combination of radiation, a downward sensible heat flux, and heat release from the soil and canopy. Biomass heat release can be an important source of energy for tall, dense forests experiencing a rapid drop in surface temperature due to evaporative cooling. Accounting for it increased E_{PM} for forest by 17%. While lateral advection of energy from nearby (dry) areas is plausible, large-scale lateral advection from a warmer ocean does not need to be invoked to explain a downward heat flux. It is not obvious how the magnitude of the downward heat flux during rainfall might be predicted, but it would likely require more explicit consideration of boundary layer dynamics.

[2] The aerodynamic component of E_{PM} is typically larger than the radiation component. Correspondingly, E_{PM} estimates are particularly sensitive to errors in air humidity and aerodynamic conductance. Small measurement errors in air humidity are plausible and important: reducing measured values by only 2% RH increased E_{PM} by an average 34%. It follows that accurately measuring RH may be particularly critical under wet conditions. Errors in the estimation of aerodynamic conductance following conventional theory were large, but did not suggest a systematic bias.

[3] FLUXNET eddy-covariance measurements of E during rainfall were questionable. In addition, rainfall is often associated with a downward heat flux, which promotes stable conditions and supresses turbulence. Our results suggest that eddy-covariance flux measurement during rainfall requires special scrutiny, and may require more flexible protocols for the analysis of raw high

frequency data. Standard FLUXNET gap-filling procedures are not appropriate under these conditions. Alternative latent heat flux estimates may be obtained from Penman-Monteith theory, but this has its own uncertainties.

[4] In addition to the various reasons why E_{PM} may be underestimated, applying rainfall interception models to canopy water budget observations can also lead to overestimates of E_{WB}. In interpreting event-based measurements, underestimation of canopy rainfall storage capacity S and overestimation of event-average rainfall rate R can lead to overestimates of E due to parameter equivalence within the rainfall interception model. The impact of assumed canopy drying time needs to be considered carefully when determining the number of storm events and their duration from rainfall rate measurements.

[5] A Rutter-type time step rainfall interception model was applied with adjusted E_{PM} estimates and assumed vegetation properties. This produced hypothetical estimates that appeared to agree surprisingly well with the magnitude of interception losses observed in field studies. Overall, therefore, careful treatment and interpretation of observations may often already be sufficient to reconcile canopy water budget measurements within a coupled water and energy balance framework. Simultaneous measurements of rainfall, throughfall and meteorology within events are likely to be helpful in this regard.

[6] Our limited understanding of boundary-layer dynamics during rainfall leaves important questions unanswered. This includes the controls on the downward heat flux, local horizontal advection, infrequent large-scale turbulence, possible upwards transport of small splash droplets, and the influence of rainfall recycling on rainfall generation downwind. These uncertainties can have important implications for coupled land surface - atmosphere modelling as well as water management, and therefore merit further study.

Acknowledgements

A.v.D. designed the methodology based on discussion with J.G., performed the analysis and wrote the first draft. J.G. and E.v.G. suggested major improvements to the argument and structure of the first draft. The other authors offered improvements to later manuscript versions.

This work used eddy-covariance data acquired by the FLUXNET community and in particular by the following networks: AmeriFlux (U.S. Department of Energy, Biological and Environmental Research, Terrestrial Carbon Program (DE-FG02-04ER63917 and DE-FG02-04ER63911), AfriFlux, AsiaFlux, CarboAfrica, CarboEuropeIP, CarboItaly, CarboMont, ChinaFlux, Fluxnet-Canada (supported by CFCAS, NSERC, BIOCAP, Environment Canada, and NRCan), GreenGrass, KoFlux, LBA, NECC, OzFlux, TCOS-Siberia, USCCC. We acknowledge the financial support to the eddy-covariance data harmonization provided by CarboEuropeIP, FAO-GTOS-TCO, iLEAPS, Max Planck Institute for Biogeochemistry, National Science Foundation, University of Tuscia, Université Laval, Environment Canada and US Department of Energy and the database development and technical support from Berkeley Water Center, Lawrence Berkeley National Laboratory, Microsoft Research eScience, Oak Ridge National Laboratory, University of California – Berkeley and the University of Virginia. We thank Dr Beverly Law and other FLUXNET members for allowing the use of their data, and for their encouragement and useful suggestions along the way. We also thank an anonymous referee and Dr David Fitzjarrald for their constructive reviews.

Appendix A. FLUXNET sites used in the analysis

We used only original (i.e. not gap-filled) half-hourly data. For each analysis we only included sites with the equivalent of more than a year of data that included observations during rainfall. The 128 FLUXNET sites with the following codes were used in some or all of the energy balance and latent heat flux analyses and/or interception modelling (primary reference between brackets, where available):

AT-Neu (Wohlfahrt et al., 2008), AU-Fog, AU-How (Beringer et al., 2011), AU-Tum (Leuning et al., 2005), AU-Wac (Kilinc et al., 2012), BE-Bra, BE-Lon, BE-Vie, BW-Ma1, CA-Ca1 (Brümmer et al., 2012), CA-Ca2 (Jassal et al., 2009), CA-Ca3 (Humphreys et al., 2006), CA-Gro (McCaughey et al., 2006), CA-Let (Flanagan and Adkinson, 2011), CA-Man (Dunn et al., 2007), CA-Mer (Lafleur et al., 2003), CA-Oas (Zha et al., 2010), CA-Obs (Krishnan et al., 2008), CA-Ojp (Kljun et al., 2006), CA-Qcu (Giasson et al., 2006), CA-Qfo (Bergeron et al., 2007), CA-SF1, -SF2 and -SF3 (Mkhabela et al., 2009), CA-TP4 (Arain and Restrepo-Coupe, 2005), CH-Oe1 (Ammann et al., 2007), CN-Du1 and -Du2 (Yan et al., 2008), CN-HaM, CN-Xfs, CN-Xi2, CZ-BK1, DE-Bay (Staudt and Foken, 2007), DE-Geb, DE-Gri, DE-Hai (Knohl et al., 2003), DE-Har, DE-Meh, DE-Tha, DE-Wet, DK-Sor (Pilegaard et al., 2011), ES-ES1, ES-VDA, FI-Hyy, FI-Kaa, FI-Sod, FR-Gri (Loubet et al., 2011), FR-Hes, FR-LBr (Berbigier et al., 2001), FR-Lq1, FR-Lq2, FR-Pue, HU-Bug (Nagy et al., 2007), HU-Mat (Pintér et al., 2010), IE-Ca1, IE-Dri (Peichl et al., 2011), IL-Yat (Rotenberg and Yakir, 2010), IS-Gun, IT-Amp, IT-BCi, IT-Col, IT-Cpz (Garbulsky et al., 2008), IT-Lav, IT-MBo (Marcolla et al., 2011), IT-Mal, IT-Non, IT-PT1 (Migliavacca et al., 2009), IT-Ren (Montagnani et al., 2009), IT-Ro1 (Rey et al., 2002), IT-Ro2 (Tedeschi et al., 2006), IT-SRo, JP-Mas, JP-Tom, KR-Hnm, NL-Ca1 (Jacobs et al., 2007), NL-Hor (Hendriks et al., 2007), NL-Loo (Moors, 2012), PT-Mi2 (Pereira et al., 2007), RU-Fyo (Milyukova et al., 2002), RU-Zot, SE-Faj (Lund et al., 2007), SE-Fla (Lindroth et al., 2008), SE-Nor (Lindroth et al., 1998), UK-ESa, UK-Gri, UK-Ham, US-ARM, US-Atq, US-Aud, US-Bkg, US-Blo, US-Bo1, US-Bo2, US-Brw, US-CaV, US-Dk1, US-Dk3, US-FPe, US-Goo, US-Ha1 (Urbanski et al., 2007), US-Ho1, US-IB1, US-IB2, US-Ivo, US-KS2, US-MMS, US-MOz, US-Me2 (Thomas et al., 2009), US-NC1 (Noormets et al., 2012), US-NC2 (Noormets et al., 2010), US-NR1, US-Ne1, US-Ne2, US-Ne3, US-SO2, US-SO3, US-SO4, US-SP2, US-SP3, US-SRM (Scott et al., 2009), US-Syv, US-Ton (Ma et al., 2007), US-UMB (Maurer et al., 2013), US-Var (Ma et al., 2007), US-WCr, US-Wi4 (Noormets et al., 2007), US-Wkg (Scott et al., 2010), and US-Wrc.

Appendix B. Canopy heat flux estimation

Michiles and Gielow (2008) found that the following approximation produced good results for Q_a (cf. McCaughey, 1985):

$$Q_a = \rho\left(c_p \Delta\overline{T} + \lambda\Delta\overline{q}\right)\frac{\Delta z}{\Delta t} \tag{B.1}$$

where $\Delta\overline{T}$ (K) and $\Delta\overline{q}$ (kg kg^{-1}) are the change in mean air temperature and specific humidity, respectively, Δz (m) the height of the air column considered and Δt (s) the time between two measurements. A similar equation describes Q_v (McCaughey, 1985; Oliphant et al., 2004; Thom, 1975; Wilson and Baldocchi, 2000):

$$Q_v = m_v c_v \frac{\Delta T_v}{\Delta t} \tag{B.2}$$

where m_v (kg m^{-2}) is the amount of fresh biomass per unit area, c_v (J kg^{-1} K^{-1}) the average specific heat, and ΔT_v (K) the average change in biomass temperature. An unknown variable in this study is T_v, given the lagged temperature changes in bulky biomass elements such as trunks and branches (e.g., Lindroth et al., 2010; Oliphant et al., 2004). Gradient methods have been developed to estimate heat storage changes in tree trunks (Meesters and Vugts, 1996) but require detailed information on the vegetation and hence were not feasible here. Alternatively, Michiles and Gielow (2008) proposed an approach that empirically estimates biomass temperature as a delayed and attenuated function of air temperature. However, it is not clear if this empirical function, developed for dry and wet, and day and night periods alike, is suitable during rainfall, when biomass surface cooling may be rapid. Instead, as a first approximation, we estimated the magnitude of biomass heat flux by applying Eq (B.2) assuming that T_v equals air temperature for intervals without rainfall, and wet bulb temperature for intervals with rainfall calculated following Stull (2011). Failure to account for the gradual release of heat may lead to overestimation of biomass heat release during the early stages of a storm, but it will to some extent be compensated by corresponding underestimation during later stages of the storm. On the other hand, biomass temperature before the storm may exceed air temperature, in which case the energy available for release will be underestimated. For c_v, values of 2466–3340 J kg^{-1} K^{-1} have been reported (Michiles and Gielow, 2008; Oliphant et al., 2004). We did not have detailed heat capacity or biomass data for each site, and therefore had to make assumptions. For an Amazonian forest, Michiles and Gielow (2008) estimated a total heat capacity of 70450 J m^{-2} K^{-1}. Dividing this by the forest height (23.5 m) suggests a biomass heat capacity per unit forest volume (i.e., biomass plus air) of 2998 J m^{-3} K^{-1}. Applying the same calculation to data presented by Kilinc et al. (2012) for an 80 m Australian mountain ash forest suggests a heat capacity of 3939 J m^{-3} K^{-1}. Based on these numbers, we estimated the product $m_v c_v$ as 3500 J m^{-2} K^{-1} per metre vegetation height. Values for these were sourced from publications or the web sites of FLUXNET and its contributing regional networks.

Appendix C. Simplified rainfall interception model

We applied the Rutter et al. (1971) rainfall interception model with four simplifying assumptions: (1) the canopy has full cover; (2) drainage of water in excess of rainfall storage capacity occurs sufficiently rapidly and therefore its influence on interception losses can be ignored at half-hourly time step, (3) the trunks behave as an integral part of the vegetation and therefore their water balance does not need to be considered separately, and (4) wet canopy evaporation is limited by the amount of water on the canopy surface (C in mm), but does not linearly scale with it. With these assumptions $C(t)$ at the end of period t is predicted as (Rutter et al., 1971; Rutter, 1975):

$$C(t) = C(t-1) + P'(t) - E'(t) \qquad \text{(C.1)}$$

with limitations $C(t) \leq S$ and $E'(t) \leq C(t\text{–}1) + P'(t)$, where P' and E' are rainfall and total wet canopy evaporation (mm) during time interval t. E' was estimated from λE_{PM} and missing values during and after rainfall were estimated as the mean λE_{PM} for all time intervals with and without rainfall, respectively. Different values of S between 0.1 and 5 mm were tested, covering a realistic range of values reported in the literature. A brief discussion of the simplifying assumptions follows.

- Assumption (1) was made to avoid mathematical inconsistencies in the model and to keep the model simple, rather than resort to partial canopy models, which require more assumptions and input data and are more cumbersome to interpret (Gash et al., 1995; Valente et al., 1997; Van Dijk and Bruijnzeel, 2001a). Canopy cover is close to unity for many of the FLUXNET sites and for those cases the impact will be minor. However, for sites with partial or seasonally varying canopy cover (e.g. open forests, crop sites) the resulting interception estimates should be considered unrealistic.
- Assumption (2) will have little influence on the results, as the rate of drainage is normally high and because rainfall storage in excess of S does not lead to greater E in the original model (Rutter et al., 1971). It is also consistent with the derivation of the event-based model by Gash (1979), who assumed that drainage from the saturated canopy would become negligible within 20 to 30 min after the end of a storm.
- Assumption (3) has a sound conceptual basis but in any case will also not substantially affect the simulated interception losses as the stemflow fraction is normally very small (Van Dijk and Bruijnzeel, 2001a; Wallace et al., 2013).
- Assumption (4) is potentially more influential. In the original model formulation E scales linearly with the ratio C/S. We did not adhere to this formulation because it would prevent the canopy from ever drying completely between storms. Moreover there is in fact little empirical support to suggest that wet canopy evaporation is linearly proportional to rainfall storage on the canopy (but see Shuttleworth, 1976; Shuttleworth, 1977). It is noted that this assumption has no effect when R

exceeds E, which generally will be the case during rainfall. To test the influence of this assumption, the model was also applied in its original form. This produced interception estimates that were only 4–5% smaller and the values were highly correlated (r^2>0.99) with values of S.

References

Amiro, B.D. et al., 2006. Carbon, energy and water fluxes at mature and disturbed forest sites, Saskatchewan, Canada. Agricultural and Forest Meteorology, 136(3–4): 237-251.

Ammann, C., Flechard, C., Leifeld, J., Neftel, A. and Fuhrer, J., 2007. The carbon budget of newly established temperate grassland depends on management intensity. Agriculture, ecosystems & environment, 121(1): 5-20.

Arain, M.A. and Restrepo-Coupe, N., 2005. Net ecosystem production in a temperate pine plantation in southeastern Canada. Agricultural and Forest Meteorology, 128(3–4): 223-241.

Aubinet, M., Vesala, T. and Papale, D., 2012. Eddy covariance: a practical guide to measurement and data analysis. Springer.

Baldocchi, D., 2008. Turner Review No. 15: 'Breathing' of the terrestrial biosphere: lessons learned from a global network of carbon dioxide flux measurement systems. Australian Journal of Botany, 56(1): 26.

Baldocchi, D. et al., 2001. FLUXNET: A New Tool to Study the Temporal and Spatial Variability of Ecosystem–Scale Carbon Dioxide, Water Vapor, and Energy Flux Densities. Bulletin of the American Meteorological Society, 82(11): 2415-2434.

Bassette, C. and Bussière, F., 2008. Partitioning of splash and storage during raindrop impacts on banana leaves. Agricultural and Forest Meteorology, 148(6): 991-1004.

Belcher, S. E., Finnigan, J. J., and Harman, I. N., 2008. Flows through forest canopies in complex terrain. Ecological Appliactions, 18: 1436–1453.

Belcher, S. E., Harman, I. N., and Finnigan, J. J., 2012. The wind in the willows: Flows in forest canopies in complex terrain. Annual Review of Fluid Mechanics, 44: 479–504.

Berbigier, P., Bonnefond, J.-M. and Mellmann, P., 2001. CO_2 and water vapour fluxes for 2 years above Euroflux forest site. Agricultural and Forest Meteorology, 108(3): 183-197.

Bergeron, O. et al., 2007. Comparison of carbon dioxide fluxes over three boreal black spruce forests in Canada. Global Change Biology, 13(1): 89-107.

Beringer, J. et al., 2011. SPECIAL—Savanna Patterns of Energy and Carbon Integrated across the Landscape. Bulletin of the American Meteorological Society, 92(11): 1467-1485.

Beven, K., 1993. Prophecy, reality and uncertainty in distributed hydrological modelling. Advances in Water Resources, 16: 41-41.

Blyth, E.M., Dolman, A.J. and Noilhan, J., 1994. The efect of forest on mesoscale rainfall: an example from HAPEX-MOBILHY. Journal of Applied Meteorology, 33(4): 445-454.

Bonan, G.B., 2008. Forests and Climate Change: Forcings, Feedbacks, and the Climate Benefits of Forests. Science, 320(5882): 1444-1449.

Brümmer, C. et al., 2012. How climate and vegetation type influence evapotranspiration and water use efficiency in Canadian forest, peatland and grassland ecosystems. Agricultural and Forest Meteorology, 153: 14-30.

Burba, G.G., McDermitt, D.K., Anderson, D.J., Furtaw, M.D. and Eckles, R.D., 2010. Novel design of an enclosed CO_2/H_2O gas analyser for eddy covariance flux measurements. Tellus B, 62(5): 743-748.

Cabral, O.M.R. et al., 2010. The energy and water balance of a Eucalyptus plantation in southeast Brazil. Journal of Hydrology, 388(3–4): 208-216.

Chen, S. et al., 2009. Energy balance and partition in Inner Mongolia steppe ecosystems with different land use types. Agricultural and Forest Meteorology, 149(11): 1800-1809.

Crockford, R.H. and Richardson, D.P., 2000. Partitioning of rainfall into throughfall, stemflow and interception: effect of forest type, ground cover and climate. Hydrological Processes, 14(16-17): 2903-2920.

Curtis, P.S. et al., 2002. Biometric and eddy-covariance based estimates of annual carbon storage in five eastern North American deciduous forests. Agricultural and Forest Meteorology, 113(1–4): 3-19.

Czikowsky, M.J. and Fitzjarrald, D.R., 2009. Detecting rainfall interception in an Amazonian rain forest with eddy flux measurements. Journal of Hydrology, 377(1-2): 92-105.

Dunin, F., O'Loughlin, E. and Reyenga, W., 1988. Interception loss from eucalypt forest: lysimeter determination of hourly rates for long term evaluation. Hydrological Processes, 2(4): 315-329.

Dunkerley, D.L., 2009. Evaporation of impact water droplets in interception processes: Historical precedence of the hypothesis and a brief literature overview. Journal of Hydrology, 376(3): 599-604.

Dunn, A.L., Barford, C.C., Wofsy, S.C., Goulden, M.L. and Daube, B.C., 2007. A long-term record of carbon exchange in a boreal black spruce forest: means, responses to interannual variability, and decadal trends. Global Change Biology, 13(3): 577-590.

Finnigan, J.J., Clement, R., Malhi, Y., Leuning, R. and Cleugh, H.A., 2003. A Re-Evaluation of Long-Term Flux Measurement Techniques Part I: Averaging and Coordinate Rotation. Boundary-Layer Meteorology, 107(1): 1-48.

Finnigan, J.J., 2004. Advection and modelling. In: Lee, X., Massman, W., Law, B. (Eds.), Handbook of Micrometeorology: A Guide for Surface Flux Measurements, Kluwer Academic Publishers, p. 209-241.

Flanagan, L.B. and Adkinson, A.C., 2011. Interacting controls on productivity in a northern Great Plains grassland and implications for response to ENSO events. Global Change Biology, 17(11): 3293-3311.

Foken, T., 2008. The energy balance closure problem: an overview. Ecological Applications, 18(6): 1351-1367.

Fratini, G., Ibrom, A., Arriga, N., Burba, G. and Papale, D., 2012. Relative humidity effects on water vapour fluxes measured with closed-path eddy-covariance systems with short sampling lines. Agricultural and Forest Meteorology, 165(0): 53-63.

Garbulsky, M.F., Peñuelas, J., Papale, D. and Filella, I., 2008. Remote estimation of carbon dioxide uptake by a Mediterranean forest. Global Change Biology, 14(12): 2860-2867.

Gash, J.H.C., 1979. An analytical model of rainfall interception by forests. Quarterly Journal of the Royal Meteorological Society, 105: 43-55.

Gash, J.H.C., Lloyd, C.R. and Lachaud, G., 1995. Estimating sparse forest rainfall interception with an analytical model. Journal of Hydrology, 170(1-4): 79-86.

Gash, J.H.C. and Shuttleworth, W.J. (Editors), 2007. Evaporation. Benchmark papers in hydrology, 2, 521 pp.

Gash, J.H.C., Valente, F. and David, J.S., 1999. Estimates and measurements of evaporation from wet, sparse pine forest in Portugal. Agricultural and Forest Meteorology, 94(2): 149-158.

Ghadiri, H. and Payne, D., 1988. The formation and characteristics of splash following raindrop impact on soil. Journal of Soil Science, 39(4): 563-575.

Giasson, M.-A., Coursolle, C. and Margolis, H.A., 2006. Ecosystem-level CO_2 fluxes from a boreal cutover in eastern Canada before and after scarification. Agricultural and Forest Meteorology, 140(1–4): 23-40.

Guerschman, J.P. et al., 2009. Scaling of potential evapotranspiration with MODIS data reproduces flux observations and catchment water balance observations across Australia. Journal of Hydrology, 369(1-2): 107-119.

Gunn, R. and Kinzer, G.D., 1949. The terminal velocity of fall for water droplets on stagnant air. Journal of Meteorology, 6(4): 243-248.

Harman, I. N., Finnigan, J. J., 2008. Scalar concentration profiles in the canopy and roughness sublayer. Boundary-Layer Meteorology, 129(3):323–351.

Haverd, V., Cuntz, M., Leuning, R. and Keith, H., 2007. Air and biomass heat storage fluxes in a forest canopy: calculation within a soil vegetation atmosphere transfer model. Agricultural and forest meteorology, 147(3): 125-139.

Hendriks, D.M.D., van Huissteden, J., Dolman, A.J. and van der Molen, M.K., 2007. The full greenhouse gas balance of an abandoned peat meadow. Biogeosciences, 4(3): 411-424.

Herbst, M., Rosier, P.T., McNeil, D.D., Harding, R.J. and Gowing, D.J., 2008. Seasonal variability of interception evaporation from the canopy of a mixed deciduous forest. Agricultural and forest meteorology, 148(11): 1655-1667.

Herwitz, S.R., 1985. Interception storage capacities of tropical rainforest canopy trees. Journal of Hydrology, 77(1): 237-252.

Hölscher, D., Kohler, L., van Dijk, A. and Bruijnzeel, L., 2004. The importance of epiphytes to total rainfall interception by a tropical montane rain forest in Costa Rica. Journal of Hydrology, 292(1-4): 308-322.

Holwerda, F., Bruijnzeel, L., Scatena, F., Vugts, H. and Meesters, A., 2012. Wet canopy evaporation from a Puerto Rican lower montane rain forest: The importance of realistically estimated aerodynamic conductance. Journal of Hydrology, 414: 1-15.

Holwerda, F., Scatena, F. and Bruijnzeel, L., 2006. Throughfall in a Puerto Rican lower montane rain forest: a comparison of sampling strategies. Journal of Hydrology, 327(3): 592-602.

Horton, R.E., 1919. Rainfall interception. Monthly Weather Review, 47(9): 603-623.

Humphreys, E.R. et al., 2006. Carbon dioxide fluxes in coastal Douglas-fir stands at different stages of development after clearcut harvesting. Agricultural and Forest Meteorology, 140(1): 6-22.

Huntingford, C., Blyth, E.M., Wood, N., Hewe, F.E., Grant, A., 1998. The effect of topopgraphy on evaporation. Boundary-Layer Meteorology, 86(3): 487-504.

Ibrom, A., Dellwik, E., Flyvbjerg, H., Jensen, N.O. and Pilegaard, K., 2007. Strong low-pass filtering effects on water vapour flux measurements with closed-path eddy correlation systems. Agricultural and Forest Meteorology, 147(3–4): 140-156.

Jacobs, C.M.J. et al., 2007. Variability of annual CO_2 exchange from Dutch grasslands. Biogeosciences, 4(5): 803-816.

Jassal, R.S., Black, T.A., Spittlehouse, D.L., Brümmer, C. and Nesic, Z., 2009. Evapotranspiration and water use efficiency in different-aged Pacific Northwest Douglas-fir stands. Agricultural and Forest Meteorology, 149(6): 1168-1178.

Kilinc, M., Beringer, J., Hutley, L.B., Haverd, V. and Tapper, N., 2012. An analysis of the surface energy budget above the world's tallest angiosperm forest. Agricultural and Forest Meteorology, 166: 23-31.

Kljun, N. et al., 2006. Response of net ecosystem productivity of three boreal forest stands to drought. Ecosystems, 9(7): 1128-1144.

Knohl, A., Schulze, E.-D., Kolle, O. and Buchmann, N., 2003. Large carbon uptake by an unmanaged 250-year-old deciduous forest in Central Germany. Agricultural and Forest Meteorology, 118(3): 151-167.

Kobayashi, H. et al., 2012. Modeling energy and carbon fluxes in a heterogeneous oak woodland: A three-dimensional approach. Agricultural and Forest Meteorology, 152(0): 83-100.

Krishnan, P. et al., 2008. Factors controlling the interannual variability in the carbon balance of a southern boreal black spruce forest. Journal of Geophysical Research: Atmospheres (1984–2012), 113(D9).

Lafleur, P.M., Roulet, N.T., Bubier, J.L., Frolking, S. and Moore, T.R., 2003. Interannual variability in the peatland-atmosphere carbon dioxide exchange at an ombrotrophic bog. Global Biogeochemical Cycles, 17(2): 1036.

Law, F., 1957. Measurement of rainfall, interception and evaporation losses in a plantation of Sitka spruce trees. IAHS Publication no, 44: 397-411.

Leuning, R., Cleugh, H.A., Zegelin, S.J. and Hughes, D., 2005. Carbon and water fluxes over a temperate Eucalyptus forest and a tropical wet/dry savanna in Australia: measurements and comparison with MODIS remote sensing estimates. Agricultural and Forest Meteorology, 129(3-4): 151–173.

Levia, D.F. and Frost, E.E., 2003. A review and evaluation of stemflow literature in the hydrologic and biogeochemical cycles of forested and agricultural ecosystems. Journal of Hydrology, 274(1-4): 1-29.

Leyton, L., Reynolds, E.R.C. and Thompson, F.B., 1967. Rainfall interception in forest and moorland. In: W.E. Sopper and H.W. Lull (Editors), Forest Hydrology. Pergamon, New York, NY, pp. 163–178.

Lindroth, A., Grelle, A. and Morén, A.-S., 1998. Long-term measurements of boreal forest carbon balance reveal large temperature sensitivity. Global Change Biology, 4(4): 443-450.

Lindroth, A., Klemedtsson, L., Grelle, A., Weslien, P. and Langvall, O., 2008. Measurement of net ecosystem exchange, productivity and respiration in three spruce forests in Sweden shows unexpectedly large soil carbon losses. Biogeochemistry, 89(1): 43-60.

Lindroth, A., Mölder, M. and Lagergren, F., 2010. Heat storage in forest biomass improves energy balance closure. Biogeosciences, 7(1): 301-313.

Llorens, P. and Domingo, F., 2007. Rainfall partitioning by vegetation under Mediterranean conditions. A review of studies in Europe. Journal of Hydrology, 335(1-2): 37-54.

Lloyd, C.R. and Marques, A., 1988. Spatial variability of throughfall and stemflow measurements in Amazonian rainforest. Agricultural and Forest Meteorology, 42(1): 63-73.

Loubet, B. et al., 2011. Carbon, nitrogen and Greenhouse gases budgets over a four years crop rotation in northern France. Plant and Soil, 343(1-2): 109-137.

Lund, M., Lindroth, A., Christensen, T.R. and Ström, L., 2007. Annual CO_2 balance of a temperate bog. Tellus B, 59(5): 804-811.

Ma, S., Baldocchi, D.D., Xu, L. and Hehn, T., 2007. Inter-annual variability in carbon dioxide exchange of an oak/grass savanna and open grassland in California. Agricultural and Forest Meteorology, 147(3): 157-171.

Marcolla, B. et al., 2011. Climatic controls and ecosystem responses drive the inter-annual variability of the net ecosystem exchange of an alpine meadow. Agricultural and Forest Meteorology 151(9): 1233-1243.

Mammarella, I. et al., 2009. Relative Humidity Effect on the High-Frequency Attenuation of Water Vapor Flux Measured by a Closed-Path Eddy Covariance System. Journal of Atmospheric and Oceanic Technology, 26(9): 1856-1866.

Maurer, K.D., Hardiman, B.S., Vogel, C.S. and Bohrer, G., 2013. Canopy-structure effects on surface roughness parameters: Observations in a Great Lakes mixed-deciduous forest. Agricultural and Forest Meteorology, 177(0): 24-34.

McCaughey, J., 1985. Energy balance storage terms in a mature mixed forest at Petawawa, Ontario—a case study. Boundary-Layer Meteorology, 31(1): 89-101.

McCaughey, J., Pejam, M., Arain, M. and Cameron, D., 2006. Carbon dioxide and energy fluxes from a boreal mixedwood forest ecosystem in Ontario, Canada. Agricultural and Forest Meteorology, 140(1): 79-96.

Meesters, A. and Vugts, H., 1996. Calculation of heat storage in stems. Agricultural and Forest Meteorology, 78(3): 181-202.

Michiles, A.A.d.S. and Gielow, R., 2008. Above-ground thermal energy storage rates, trunk heat fluxes and surface energy balance in a central Amazonian rainforest. Agricultural and Forest Meteorology, 148(6–7): 917-930.

Migliavacca, M. et al., 2009. Seasonal and interannual patterns of carbon and water fluxes of a poplar plantation under peculiar eco-climatic conditions. Agricultural and Forest Meteorology, 149(9): 1460-1476.

Milyukova, I.M. et al., 2002. Carbon balance of a southern taiga spruce stand in European Russia. Tellus B, 54(5): 429-442.

Miralles, D.G., Gash, J.H., Holmes, T.R.H., de Jeu, R.A.M. and Dolman, A., 2010. Global canopy interception from satellite observations. Journal of Geophysical Research, 115(D16): D16122.

Mizutani, K., Yamanoi, K., Ikeda, T. and Watanabe, T., 1997. Applicability of the eddy correlation method to measure sensible heat transfer to forest under rainfall conditions. Agricultural and forest meteorology, 86(3): 193-203.

Mkhabela, M.S. et al., 2009. Comparison of carbon dynamics and water use efficiency following fire and harvesting in Canadian boreal forests. Agricultural and Forest Meteorology, 149(5): 783-794.

Moffat, A.M. et al., 2007. Comprehensive comparison of gap-filling techniques for eddy covariance net carbon fluxes. Agricultural and Forest Meteorology, 147(3-4): 209-232.

Montagnani, L. et al., 2009. A new mass conservation approach to the study of CO_2 advection in an alpine forest. Journal of Geophysical Research: Atmospheres (1984–2012), 114(D7).

Monteith, J.L., 1981. Evaporation and surface temperature. Quarterly Journal of the Royal Meteorological Society, 107(451): 1-27.

Moors, E.J., 2012. Water use of forests in the Netherlands. PhD Thesis,. VU University Amsterdam, Amsterdam.

Murakami, S., 2006. A proposal for a new forest canopy interception mechanism: Splash droplet evaporation. Journal of Hydrology, 319(1-4): 72-82.

Muzylo, A. et al., 2009. A review of rainfall interception modelling. Journal of Hydrology, 370(1-4): 191-206.

Nagy, Z. et al., 2007. The carbon budget of semi-arid grassland in a wet and a dry year in Hungary. Agriculture, ecosystems & environment, 121(1): 21-29.

Noormets, A., Chen, J. and Crow, T., 2007. Age-Dependent Changes in Ecosystem Carbon Fluxes in Managed Forests in Northern Wisconsin, USA. Ecosystems, 10(2): 187-203.

Noormets, A. et al., 2010. Response of carbon fluxes to drought in a coastal plain loblolly pine forest. Global Change Biology, 16(1): 272-287.

Noormets, A. et al., 2012. The role of harvest residue in rotation cycle carbon balance in loblolly pine plantations. Respiration partitioning approach. Global Change Biology, 18(10): 3186-3201.

Oliphant, A. et al., 2004. Heat storage and energy balance fluxes for a temperate deciduous forest. Agricultural and Forest Meteorology, 126(3): 185-201.

Paulson, C.A., 1970. The mathematical representation of wind speed and temperature profiles in the unstable atmospheric surface layer. Journal of Applied Meteorology, 9(6): 857-861.

Peichl, M., Leahy, P. and Kiely, G., 2011. Six-year Stable Annual Uptake of Carbon Dioxide in Intensively Managed Humid Temperate Grassland. Ecosystems, 14(1): 112-126.

Penman, H., 1952. The physical bases of irrigation control, 13th International hort. Congress. London.

Pereira, F., Gash, J., David, J. and Valente, F., 2009. Evaporation of intercepted rainfall from isolated evergreen oak trees: Do the crowns behave as wet bulbs? Agricultural and Forest Meteorology, 149(3): 667-679.

Pereira, J.S. et al., 2007. Net ecosystem carbon exchange in three contrasting Mediterranean ecosystems – the effect of drought. Biogeosciences, 4(5): 791-802.

Pilegaard, K., Ibrom, A., Courtney, M.S., Hummelshøj, P. and Jensen, N.O., 2011. Increasing net CO_2 uptake by a Danish beech forest during the period from 1996 to 2009. Agricultural and Forest Meteorology, 151(7): 934-946.

Pintér, K., Balogh, J. and Nagy, Z., 2010. Ecosystem scale carbon dioxide balance of two grasslands in Hungary under different weather conditions. Acta Biologica Hungarica, 61: 130-135.

Raupach, M.R., Weng, W.S., Carruthers, D.J., Hunt, J.C.R., 1992. Temperature and humidity fields and fluxes over low hills. Quarterly Journal of the Royal Meteorological Society 118(504), 191-225.

Raupach, M. R., Finnigan, J. J., and Brunet, Y., 1996. Coherent eddies and turbulence in vegetation canopies: the mixing length analogy. Boundary-Layer Meteorology, 78:351–382.

Raupach, M.R., Finnigan, J.J., 1997. The influence of topography on meteorology variables and surface-atmosphere interactions. Journal of Hydrology, 190, 182–213.

Rebmann, C. et al., 2005. Quality analysis applied on eddy covariance measurements at complex forest sites using footprint modelling. Theoretical and Applied Climatology, 80(2-4): 121-141.

Rey, A. et al., 2002. Annual variation in soil respiration and its components in a coppice oak forest in Central Italy. Global Change Biology, 8(9): 851-866.

Richardson, A.D. et al., 2006. A multi-site analysis of random error in tower-based measurements of carbon and energy fluxes. Agricultural and Forest Meteorology, 136(1–2): 1-18.

Roberts, J., 1999. Plants and water in forests and woodlands, Ecohydrology. Routledge, London, UK.

Roberts, J.M., Gash, J.H.C., Tani, M. and Bruijnzeel, L.A., 2005. Controls on evaporation in lowland tropical rainforest. In: M. Bonell and L.A. Bruijnzeel (Editors), Forests, Water and People in the Humid Tropics: Past, Present and Future Hydrological Research for Integrated Land and Water Management. Cambridge University Press, Cambridge, pp. 287-313.

Ross, A.N., 2011. Scalar transport over forested hills. Boundary-Layer Meteorology, 141:179–199.

Rotenberg, E. and Yakir, D., 2010. Contribution of Semi-Arid Forests to the Climate System. Science, 327(5964): 451-454.

Rutter, A., Kershaw, K., Robins, P. and Morton, A., 1971. A predictive model of rainfall interception in forests, 1. Derivation of the model from observations in a plantation of Corsican pine. Agricultural Meteorology, 9: 367-384.

Rutter, A.J. (Editor), 1967. An analysis of evaporation from a stand of Scots pine. International Symposium on Forest Hydrology. Pergamon Press, Oxford, UK, 403-416 pp.

Rutter, A.J., 1975. The hydrological cycle in vegetation. In: J.L. Monteith (Editor), Vegetation and the atmosphere: Volume 1, Principles. Academic Press: London, pp. 111–154.

Sakai, R.K., Fitzjarrald, D.R. and Moore, K.E., 2001. Importance of Low-Frequency Contributions to Eddy Fluxes Observed over Rough Surfaces. Journal of Applied Meteorology, 40(12): 2178-2192.

Schellekens, J., Scatena, F.N., Bruijnzeel, L.A. and Wickel, A.J., 1999. Modelling rainfall interception by a lowland tropical rain forest in northeastern Puerto Rico. Journal of Hydrology, 225(3-4): 168-184.

Schmidt, A., Hanson, C., Chan, W.S. and Law, B.E., 2012. Empirical assessment of uncertainties of meteorological parameters and turbulent fluxes in the AmeriFlux network. Journal of Geophysical Research: Biogeosciences, 117(G4): G04014.

Scott, R.L., Hamerlynck, E.P., Jenerette, G.D., Moran, M.S. and Barron-Gafford, G.A., 2010. Carbon dioxide exchange in a semidesert grassland through drought-induced vegetation change. Journal of Geophysical Research: Biogeosciences (2005–2012), 115(G3).

Scott, R.L., Jenerette, G.D., Potts, D.L. and Huxman, T.E., 2009. Effects of seasonal drought on net carbon dioxide exchange from a woody-plant-encroached semiarid grassland. Journal of Geophysical Research: Biogeosciences (2005–2012), 114(G4).

Sevruk, B., 2006. Rainfall Measurement: Gauges, Encyclopedia of Hydrological Sciences. John Wiley & Sons, Ltd.

Shuttleworth, W.J., 1976. Experimental evidence for the failure of the Penman-Monteith equation in partially wet conditions. Boundary-Layer Meteorology, 10(1): 91-94.

Shuttleworth, W.J., 1977. Comments on 'resistance of a partially wet canopy: Whose equation fails?'. Boundary-Layer Meteorology, 12(3): 385-386.

Shuttleworth, W.J., 2012. Terrestrial hydrometeorology. John Wiley & Sons.

Shuttleworth, W.J. and Calder, I.R., 1979. Has the Priestley-Taylor equation any relevance to forest evaporation? Journal of Applied Meteorology, 18(5): 639-646.

Staudt, K. and Foken, T., 2007. Documentation of reference data for the experimental areas of the Bayreuth Centre for Ecology and Environmental Research (BayCEER) at the Waldstein site. Arbeitsergebnisse, 35. Universität Bayreuth, Abt. Mikrometeorologie, ISSN 1614-8916, Bayreuth, Germany, 35 pp.

Stewart, J.B., 1977. Evaporation from the wet canopy of a pine forest. Water Resources Research, 13(6): 915-921.

Stoy, P.C. et al., 2006. An evaluation of models for partitioning eddy covariance-measured net ecosystem exchange into photosynthesis and respiration. Agricultural and Forest Meteorology, 141(1): 2-18.

Stoy, P.C. et al., 2013. A data-driven analysis of energy balance closure across FLUXNET research sites: The role of landscape scale heterogeneity. Agricultural and forest meteorology, 171: 137-152.

Stull, R., 2011. Wet-Bulb Temperature from Relative Humidity and Air Temperature. Journal of Applied Meteorology and Climatology, 50(11): 2267-2269.

Tedeschi, V. et al., 2006. Soil respiration in a Mediterranean oak forest at different developmental stages after coppicing. Global Change Biology, 12(1): 110-121.

Thom, A.S., 1975. Momentum, Mass and Heat Exchange of Plant Communities. In: J.L. Monteith (Editor), Vegetation and the Atmosphere. Academic Press, London, pp. 57-109.

Thomas, C.K. et al., 2009. Seasonal hydrology explains interannual and seasonal variation in carbon and water exchange in a semiarid mature ponderosa pine forest in central Oregon. Journal of Geophysical Research: Biogeosciences (2005–2012), 114(G4).

Urbanski, S. et al., 2007. Factors controlling CO_2 exchange on timescales from hourly to decadal at Harvard Forest. Journal of Geophysical Research: Biogeosciences (2005–2012), 112(G2).

Valente, F., David, J.S. and Gash, J.H.C., 1997. Modelling interception loss for two sparse eucalypt and pine forests in central Portugal using reformulated Rutter and Gash analytical models. Journal of Hydrology, 190(1–2): 141-162.

Van der Tol, C., Gash, J.H.C., Grant, S.J., McNeil, D.D. and Robinson, M., 2003. Average wet canopy evaporation for a Sitka spruce forest derived using the eddy correlation-energy balance technique. Journal of Hydrology, 276(1-4): 12-19.

Van Dijk, A.I.J.M. and Bruijnzeel, L.A., 2001a. Modelling rainfall interception by vegetation of variable density using an adapted analytical model. Part 1. Model description. Journal of Hydrology, 247(3-4): 230-238.

Van Dijk, A.I.J.M. and Bruijnzeel, L.A., 2001b. Modelling rainfall interception by vegetation of variable density using an adapted analytical model. Part 2. Model validation for a tropical upland mixed cropping system. Journal of Hydrology, 247(3-4): 239-262.

Van Dijk, A.I.J.M., Peña-Arancibia, J.L. and Bruijnzeel, L.A., 2012. Land cover and water yield: inference problems when comparing catchments with mixed land cover. Hydrology and Earth System Sciences, 16(9): 3461-3473.

Van Dijk, A.I.J.M. and Warren, G.A., 2010. AWRA Technical Report 4. Evaluation Against Observations, WIRADA / CSIRO Water for a Healthy Country Flagship, Canberra.

Wallace, J. et al., 2013. Evaluation of forest interception estimation in the continental scale Australian Water Resources Assessment–Landscape (AWRA-L) model. Journal of Hydrology, 499: 210-223.

Wallace, J. and McJannet, D., 2006. On interception modelling of a lowland coastal rainforest in northern Queensland, Australia. Journal of Hydrology, 329(3): 477-488.

Wang, W., Liang, S. and Meyers, T., 2008. Validating MODIS land surface temperature products using long-term nighttime ground measurements. Remote Sensing of Environment, 112(3): 623-635.

Williams, C.A. et al., 2012. Climate and vegetation controls on the surface water balance: Synthesis of evapotranspiration measured across a global network of flux towers. Water Resources Research, 48(6).

Wilson, K. et al., 2002. Energy balance closure at FLUXNET sites. Agricultural and Forest Meteorology, 113(1-4): 223-243.

Wilson, K.B. and Baldocchi, D.D., 2000. Seasonal and interannual variability of energy fluxes over a broadleaved temperate deciduous forest in North America. Agricultural and Forest Meteorology, 100(1): 1-18.

Wohlfahrt, G. et al., 2008. Seasonal and inter-annual variability of the net ecosystem CO_2 exchange of a temperate mountain grassland: Effects of weather and management. Journal of Geophysical Research: Atmospheres, 113(D8): D08110.

Yan, Y. et al., 2008. Closing the carbon budget of estuarine wetlands with tower-based measurements and MODIS time series. Global Change Biology, 14(7): 1690-1702.

Zha, T. et al., 2010. Interannual variation of evapotranspiration from forest and grassland ecosystems in western Canada in relation to drought. Agricultural and Forest Meteorology, 150(11): 1476-1484.

Table 1. Measured energy balance for tall and short vegetation, during periods with and without rainfall, respectively. Listed are mean net radiation (R_n), ground heat flux (G), eddy-covariance derived sensible (H_{EC}) and latent heat flux (λE_{EC}), as well as the energy balance residual between the four terms and the energy balance ratio (EBR), the latter calculated as the ratio $(\lambda E+H) / (Rn–G)$. Heat storage in the canopy was not considered in this case. Mean values were calculated as the simple mean for half-hourly intervals with and without precipitation at each site (based on a 0.25 mm threshold). Numbers listed represent the mean and standard deviation across sites with tall vegetation (>3 m) and short vegetation (<1.5 m), respectively (20 out of 128 sites has intermediate vegetation height or lacked sufficient data and were not included). Positive and negative signs here follow FLUXNET conventions (i.e., upward and downward, respectively).

		R_n	G	H_{EC}	λE_{EC}	Residual	EBR
		W m^{-2}	W m^{-2}	W m^{-2}	W m^{-2}	W m^{-2}	-
tall vegetation	dry	89 ± 24	-1 ± 2	35 ± 21	37 ± 15	16 ± 13	0.80 ± 0.16
(>3 m, N=59)	rainfall	31 ± 21	2 ± 8	-12 ± 16	17 ± 15	28 ± 20	-0.37 ± 1.92
short vegetation	dry	70 ± 26	-1 ± 3	20 ± 17	38 ± 18	11 ± 13	0.86 ± 0.32
(<1.5 m, N=49)	rainfall	23 ± 18	6 ± 11	-6 ± 8	17 ± 14	18 ± 17	0.36 ± 0.56

Table 2. Proposed explanations for the discrepancy between wet canopy evaporation (E) inferred through the water budget method and conventional Penman-Monteith approach (E_{PM}). The implications for E_{PM} and water budget derived interception loss (I) are indicated.

Proposed explanation	Implication	
	E_{PM} correct	I correct
Errors in applying Penman-Monteith theory		
Energy advection not accounted for	unclear	yes
Biomass heat release underestimated	no	yes
Errors in air humidity measurement	no	yes
Aerodynamic conductance underestimated	no	yes
Mechanical transport not accounted for	yes	yes
Errors in applying rainfall interception models		
Canopy storage capacity underestimated	yes	yes
Rainfall rate overestimated	yes	yes

Table 3. Estimated energy balance during rainfall for tall and short vegetation. For comparison, eddy-covariance based values reported in the FLUXNET database are also listed. Values were calculated as in Table 1, but in addition to H and λE values reported in the FLUXNET database (subscript 'EC') were also calculated using the Penman-Monteith equation with best available inputs ('PM') and the more conventional application ('PMo'), both described in the text (all are in W m^{-2}). Meaning of symbols is as in Table 1, but positive and negative numbers here indicate incoming energy (gains) and outgoing energy (losses), respectively. The number of sites is slightly smaller than those used in Table 1 due to data availability.

	R_n	G	Q	H_{PM}	λE_{PM}	H_{EC}	λE_{EC}	λE_{PMo}
tall vegetation (>3 m, *N*=57)	31 ± 22	2 ± 8	29 ± 31	39 ± 40	-102 ±94	12 ± 17	-17 ± 15	-93 ± 84
short vegetation (<1.5 m, *N*=46)	24 ± 18	7 ± 11	1 ± 1	17 ± 20	-48 ± 28	5 ± 9	-18 ± 14	-47 ± 26

Table 4. Mean wet canopy evaporation rate (E) and rainfall rate (R) and their ratio $\overline{E}/\overline{R}$ as calculated from the simulation results for 83 sites using an intermediate canopy rainfall storage capacity estimate of S=1 mm.

	rainfall half-hours	*event-average*	*drying out phase*
mean E (mm h^{-1})	0.15 ± 0.13	0.17 ± 0.11	0.33 ± 0.17
mean R (mm h^{-1})	1.62 ± 0.82	1.04 ± 0.63	
mean E / mean R	0.11 ± 0.11	0.19 ± 0.12	

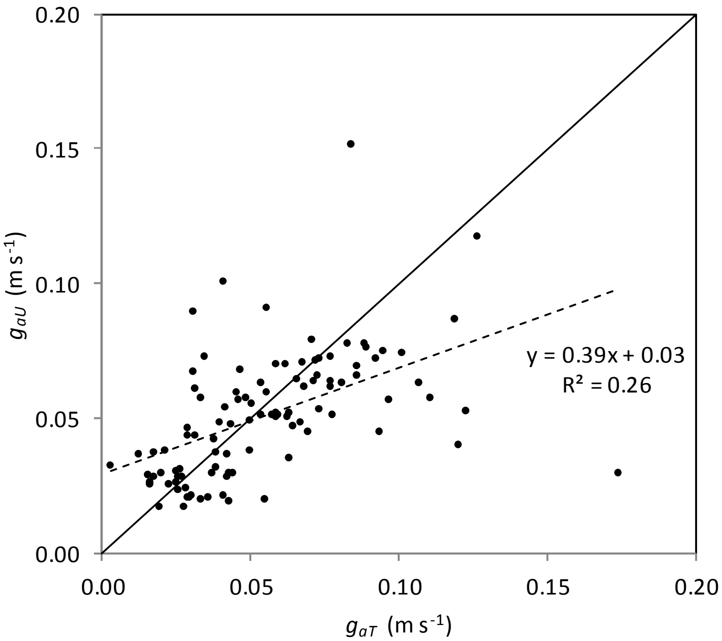

Figure 1. Comparison between aerodynamic conductance during rainfall calculated from measured friction velocity (g_{aU}) and estimated following Thom (g_{aT}) for all vegetation types (N=102).

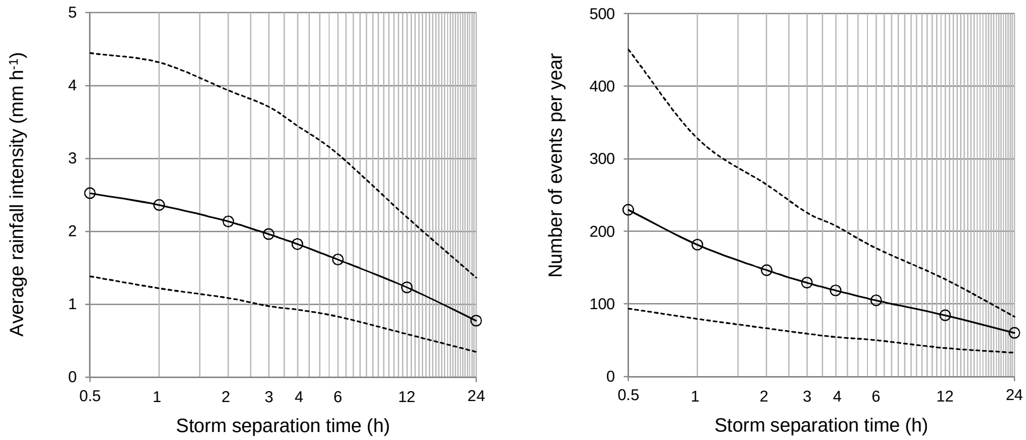

Figure 2. Relationship between storm separation time and (a) mean event-average rainfall rate (*R*) and (b) number of rainfall events per year. Solid line represents mean of all sites, dotted lines show the 90% range (*N*=184).

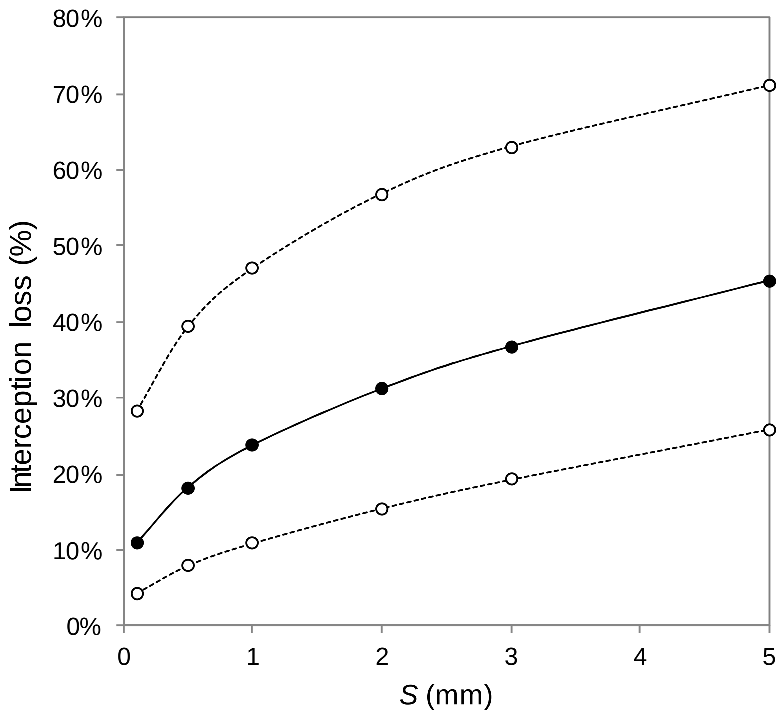

Figure 3. Influence of canopy rainfall storage capacity (*S*) on interception loss (% of rainfall) simulated with the simplified model of Rutter et al. (1971). Solid line and circle shows average for 82 sites; open dots and dashed lines bound the 90% range.

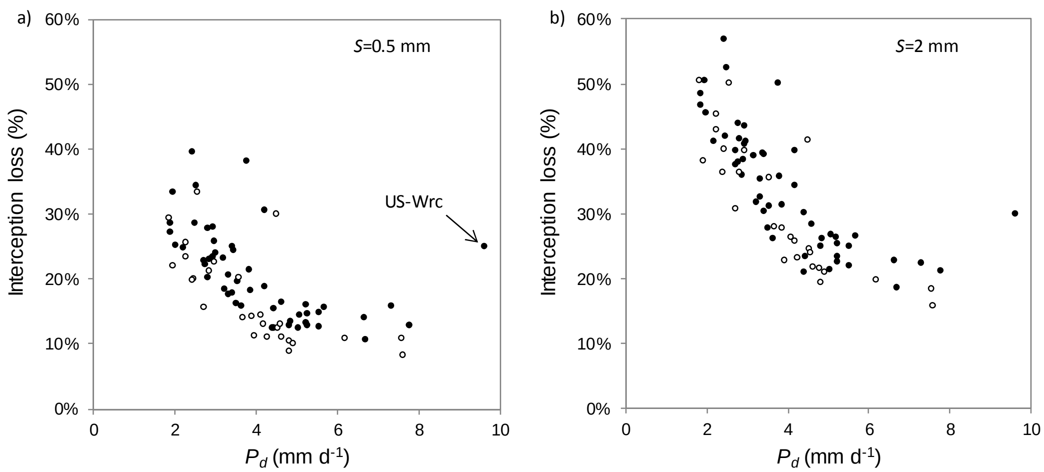

Figure 4. Relationship between the average precipitation per rain day (P_d) and model-simulated rainfall interception loss (% of rainfall) for 83 FLUXNET sites. Interception was simulated using a simplified version of the model of Rutter et al. (1971) by assuming a canopy storage capacity (S) of (a) 0.5 mm and (b) 2 mm. Open circles are for short vegetation (<1.5 m), solid circles for tall vegetation (>3 m).